**Advances in Materials**
2019; 8(4): 142-155
http://www.sciencepublishinggroup.com/j/am
doi: 10.11648/j.am.20190804.13
ISSN: 2327-2503 (Print); ISSN: 2327-252X (Online)

# Environmentally Benign All-inorganic Perovskite Solar Cells

**Liqiu Zheng[1, *], Robert S. Owor[2], Zhongrui Li[3]**

[1]Chemistry and Forensic Sciences Department, Albany State University, Albany, USA

[2]Mathematics and Computer Sciences Department, Albany State University, Albany, USA

[3]Electron Microbeam Analysis Laboratory, University of Michigan, Ann Arbor, USA

**Email address:**
Liqiu.zheng@asurams.edu (Liqiu Zheng)

[*]Corresponding author

**To cite this article:**
Liqiu Zheng, Robert S. Owor, Zhongrui Li. Environmentally Benign All-inorganic Perovskite Solar Cells. *Advances in Materials.* Vol. 8, No. 4, 2019, pp. 142-155. doi: 10.11648/j.am.20190804.13

**Received**: September 19, 2019; **Accepted**: September 29, 2019; **Published**: October 14, 2019

**Abstract:** Organic/inorganic hybrid lead halide perovskite solar cells have recently emerged as the forerunner in the next generation of photovoltaic technology due to unprecedented progress in power conversion efficiency from their debut of 3.8% in 2009 to the currently certified 23.3%. Mixed PSC solar cells are subject to compositional degradation when exposed to ambient surroundings, which thwarts their real-world applications. Moreover, lead-based compounds pose environmental/health hazards. Very recently, all-inorganic lead-free perovskites have attracted enormous attention because this type successfully dismantles two roadblocks—instability and toxicity, which would accelerate the commercialization. In this outlook, we offered our perspective on the most recent developments in material sciences of halides all inorganic perovskites with possible alternatives to lead, the synthesis approaches, assessment of various device configurations and their progress in solar cells. For the sake of comparison, we also reviewed some all-inorganic but lead-based counterparts in order to motivate researchers to explore all the potentials. Surveying recent developments toward lead-free all-inorganic perovskite solar cells would offer a roadmap for developing new materials and navigate uncharted territory in solar energy fields.

**Keywords:** Perovskite Solar Cell, Power Conversion Efficiency, n-i-p Junction, Tandem, Up/Down Conversion, Intermediate Band

## 1. Introduction

In a world seeking cost effective, easily processable, efficient and versatile solar cells to mitigate the energy crisis, the rise of solar cell materials called perovskites has excited the photovoltaic research community because their efficiency at converting sunlight into electricity has soared from their debut of 3.8% in 2009 [1] to the currently certified 23.3% [2]. The newly emerging perovskite solar cell (PSC) rapidly outperformed the well-established technologies such as multi-crystalline Si (21.3%) and Copper Indium Gallium Selenide (CIGS, 22.3%) cells in such a short time [3], not only because of their phenomenal optoelectronic properties and the scalable popular solution processablity but also the diversity in device architectures with ease of fabrication. Therefore, it has been claimed that the advent of PSCs has broken the dawn of a new era in optoelectronic technologies. In spite of their tantalizing prospects, organic-inorganic hybrid halide PSCs are subject to compositional degradation when exposed to ambient surroundings. To date, the most reported organic-inorganic lead halide perovskite $CH_3NH_3PbI_3$ ($MAPbI_3$, $CH_3NH_3$=MA, can be replaced with $CH(NH_2)_2$=FA; X=Cl, Br or I), is also the record holder with 23.3% power conversion efficiency (PCE). The fast and irreversible degradation of $MAPbI_3$ confines virtually all measurements to a well-sealed nitrogen-filled glove box. Meanwhile, the toxicity of lead-based compounds further necessitates the pursuit of alternatives beyond $MAPbI_3$. Therefore, identifying the right ingredients for perovskite to achieve ideal photo-electronic properties and strengthen stability, at no cost to the environment, has proven a compelling challenge. In this review, we summarized the

photovoltaic studies on the possible avenues to tackle the instability and toxicity of PSCs including alternatives to lesser lead or lead-free stabilized perovskites, synthesis approaches, assessment of various device configurations and their photovoltaic (PV) performance. In the meantime, the potential development trend was envisioned to inspire the new material discovery and novel design for devices.

## 2. Materials for All Inorganic Perovskites

Perovskite, developed initially as sensitizers in dye-sensitized solar cells [1], was named after Russian mineralogist Perovski, who first characterized the crystal structure of $ABX_3$. Actually, a large family of compounds, with the same formula, can be called perovskites, which typically have unit cells composed of five atoms in a cubic structure [4], where A and B are 12- and 8-coordinates cations, located at the cube corners and body-centered positions, respectively, and X (X=halogen or oxygen) is the anion at the face-center positions, as depicted in Figure 1. A wide variety of elements with different valence can be incorporated, so long as charge neutrality is satisfied. The Goldschmidt tolerance factor (GTF) [5], t, has been extensively adopted to map the formability of halide perovskites based on the chemical formula $ABX_3$ and the ionic radii $r_i$ of each ion (A, B, X), where $t=\frac{R_A+R_X}{\sqrt{2}(R_B+R_X)}$. When $t>1$, perovskite materials tend to form a hexagonal structure; when $1>t>0.8$, the preferential structure is cubic; while if $t<0.8$, an orthorhombic structure is readily formed. To further clarify the formability/stability of $ABX_3$ perovskites, a (t, u) map is introduced [6], where u is the octahedral factor of the ratio of the B-site cation ($R_B$) and the X-site anion (Rx). Based on the existing perovskites, a simple empirical measure for stable $ABX_3$ perovskite is concluded that t must be within $0.7<t<1.107$, and $0.377<u<0.895$. Other than the tolerance/octahedral factor, the ionization energy of the cation, dimensional phases of perovskite materials, valence band and so on, also play parts in the formability and stability of perovskite structures. By varying temperature, the structure undergoes structural change even with the same chemical compositions. Take $MABX_3$ as an example, at lower temperature, $MABX_3$ forms in an orthorhombic phase (space group *pnma*) successively transforming into a tetragonal (space group: *I4/m*) and cubic structure (space group $pm\bar{3}m$) when increasing temperature.

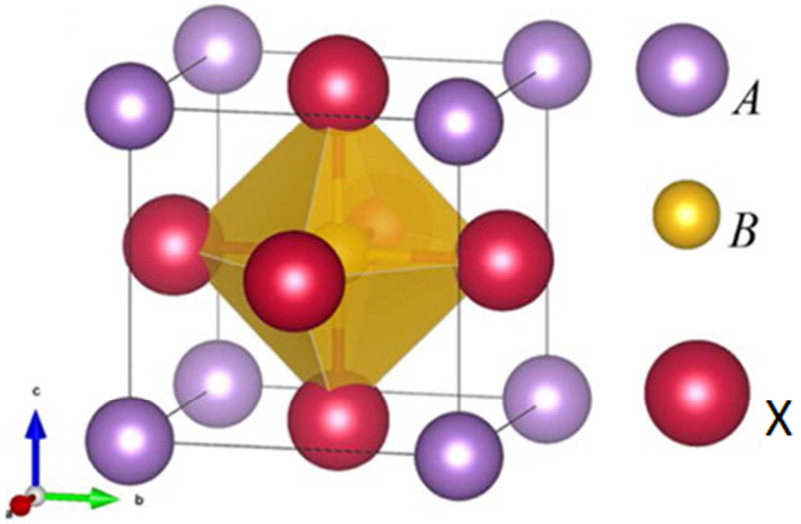


***Figure 1.*** *The diagram of crystal structure of Perovskite. Reproduced with permission [4]. Copyright 2015, American Chemical Society.*

### *2.1. On a Site*

As aforementioned, the best performing perovskite solar cells are the organic-inorganic hybrid halide compounds. The instability of this mixed type presents a challenging issue for practical applications. Addressing fragility and achieving long term stability entails replacement of the notoriously volatile organic component in the hybrid PSCs with an inorganic substitute. In particular, MA or FA is very sensitive to moisture/oxygen due to their high hygroscopicity. Inorganic monovalent alkali cations stand out as substitutes due to their stability in ambient surroundings. The tolerance factor calculations show almost all monovalent cations (for instance, the alkali metals ($Li^+$, $Na^+$, $K^+$)) are mismatched to sustain a photoactive $ABX_3$ perovskite because of their smaller size. When compared with $MA^+$ (1.80 Å) *or* FA + (1.90 Å), the $Cs^+$ (1.67 Å) and $Rb^+$ (1.52 Å) cations have smaller ionic radii, however, their GTF, for $APbI_3$, are within the proper range for stable perovskites. Additionally, since they are oxidation-stable monovalent cations, $Cs/RbPbX_3$ (as well as $MAPbX_3$ and $FAPbX_3$) falls into the well-established perovskites. The substitution $Cs^+$ for the larger organic cations leads to an octahedral tilting, accordingly widening the bandgap from 1.50 eV to 1.73 eV in $CsPbI_3$ with a cubic phase (1.7% efficiency) [7], while $CsPbI_3$ with an orthorhombic structure has an even wider bandgap of 3.0 eV. As far as the PV performance is concerned, $CsPbI_3$ with a cubic structure turns out to be the most reported inorganic lead based perovskite, due to its suitable bandgap and the dramatically improved thermal stability [8]. Some reports [9-

10] indicate that the inclusion of $Rb^+$ leads to the formation of non-perovskite structure since its size is too small to stabilize the perovskite lattice.

Theoretical calculation [11] also shows thallium ion ($Tl^+$, $4f^{14}5d^{10}6s^2$) could replace $MA^+$ to form $TlPbI_3$ with a band gap of 1.33eV based on the Density Functional Theory (DFT). The density of states of $TlPbI_3$ suggests a stronger bond exists between Tl and I, leading to lower total energy and higher stability compared to $CsPbI_3$, while the carrier concentration in both are comparable from -20°C to 50°C. However, no experimental result has been reported on $TlPbI_3$ yet.

### *2.2. On b Site Alternatives to Lead*

The best performance of lead halide perovskites is attributed to the superior and unique photovoltaic properties such as extremely high optical absorption coefficients, balanced electron and hole mobility, super-long photo-generated carrier diffusion lengths and life times, low trap densities, small exciton binding energy, ultra-small Urback energies [12-13], and so on. These phenomenal optoelectronic properties of them bear similarities to the gold standards of the widely commercialized silicon based SCs, which feature by an appropriate band gap; the extremely high optical absorption coefficient; the long-lived photo-generated electrons/holes with long diffusion lengths and balanced electron-hole transport, etc. These characteristics explain why the newly emerging PSCs are superior to the well-established PV technologies [14].

Pb, as a heavy element, has unique atomic electronic configuration-- the lone pair Pb $6s^2$, inactive Pb $6p^0$, and a strong spin-orbit coupling (SOC) caused by the large size and heavy mass. Theoretical calculations [15] indicated that exceptional photovoltaic properties of lead halide perovskite, particularly extremely high optical absorption coefficients and long carriers lifetimes and diffusion lengths, stem from the electronic states of lone pair Pb $6s^2$ and inactive Pb $6p^0$. The transition matrix elements and the joint density of state (JDOS) determine the optical absorption of a semiconductor. As a comparison, the silicon-based light absorber is an indirect bandgap semiconductor with optical absorption close to the band edge from the Si p orbital to the Si p and s orbitals. The bandgap of $MAPbI_3$, for instance, is direct, leading to stronger optical absorption. In contrast with GaAs in which the electronic structures of them are very different. The lower conduction band (LCB) of GaAs is derived from the dispersive Ga 4s states, while the LCB of $MAPbI_3$ primarily consists of Pb 6p states. The atomic p orbitals exhibit less dispersion than s orbitals do, leading to a higher JDOS in halide perovskites. Therefore, the stronger optical absorption coefficient of $MAPbI_3$ is seen up to 1 order of magnitude higher than that of GaAs within the visible light range. Visible light accounts for the major portion of the full solar spectrum. High absorption in this portion is critical to determine high efficiency solar cells. It is no surprise that the Pb halide perovskites ($MAPbI_3$ and $CsPbI_3$) outperform GaAs, $CuInSe_2$ (CIS) and $Cu_2ZnSnSe_4$ (CZTSe) for any given thickness in conversion efficiencies. It is noteworthy that the halide perovskites with very thin layer (0.3mm, for $MAPbI_3$) could achieve much higher efficiency (21%) than that of GaAs-based solar cells (13%).

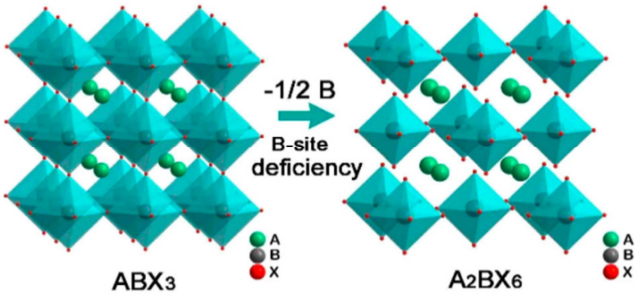


***Figure 2.*** *Schematic illustration of the transformation between the Perovskite Crystal Structures of $ABX_3$ and B-Site deficient $A_2B\square X_6$. Reproduced with permission [21]. Copyright 2018, American Chemical Society.*

Despite phenomenal performance, Pb-based halide perovskites pose hazards to the environment and human health. In order to lessen the toxicity, the most obvious option for Pb replacement is to adopt another group 14 metal, such as $Sn^{2+}$, $Ge^{2+}$. Owing to their optical band gaps in the red-infrared and good charge carriers mobility's [16], it seems that Sn-based halide perovskites hold great promise of opto-electric applications. Mathews et al [17-18] attempted $CsSnI_3$ and $CsSnI_{3-x}Br_x$ as a light absorber. The very small band gap of 1.27eV of $CsSnI_3$, resulting in a near-infrared light absorption onset to 950 nm, achieves relatively high $J_{sc}$ values up to 27.67 $mA/cm^2$, but the efficiency is still mediocre, at 3.56% [19]. Whereas, the organic-inorganic counterpart $FASnI_3$, possessing a closer optimal band gap for single junction solar cells of 1.41 eV, has achieved 7.14% [20]. Although $CsSnI_3$ does not have desirable PV performance, it lays the foundation for the Sn-based halide perovskites derivatives with $A_2SnX_6$, which demonstrate good stability in air and moisture due to the Sn in its +4 oxidation stable state. These compounds can be viewed as cubic double perovskites $Cs_2Sn_2X_6$ by removing half of the octahedral Sn atoms to form so called "vacancy ordered" double perovskites indicated as $Cs_2Sn^{4+}\square\square X_6$($\square$ represents vacancy) [21], as portrayed in Figure 2. Since they are reminiscent of molecular crystals, fascinatingly, unusually dispersive electronic band structures are exhibited by these materials with a direct band gap as low as 1.3 eV in the case of $Cs_2Sn_2I_6$ [22].

For Ge-based perovskites, most of them are still limited to theoretical simulation. For instance, $CsGeI_3$, the calculated band gap of 1.6 eV, is the lowest one among $AGeI_3$ compounds. However, theoretical studies also show that Ge vacancies in $CsGeI_3$ are the dominate defects with shallow transition levels and rather low formation enthalpy, yielding a very high hole density, which is detrimental to the photovoltaic performance [23]. To our best knowledge, the most recently reported Ge-based all inorganic perovskites, albeit, with partial replacement of Pb, was attained by Yang

et al [24]. They reported that after the introduction of $Ge^{2+}$, the phase stability of the all inorganic perovskite is enhanced. Meanwhile, the decent PCE of 10.8 % with high open circuit voltage (VOC) of 1.27 V in a planar solar cell based on $CsPb_{0.8}Ge_{0.2}I_2Br$ perovskite was achieved.

Apparently, the PV performance of substitution group 14 metals for Pb needs further improvement. At the same time, the replacement of 14 group metals with Pb in halide perovskites exacerbates the instability since they are prone to self-doping effects and structural instabilities, owing to the known tendency of oxidization from divalent $Sn^{2+}$/$Ge^{2+}$ to tetravalent $Sn^{4+}$/$Ge^{4+}$. Consequentially, solar devices tend to degrade rapidly upon exposure to surroundings. Moreover, it is unclear whether Sn would be safer than Pb because one of the degradation products, $SnI_2$, may be as harmful as its lead analogue $PbI_2$.

Very recently, $Mn^{2+}$ has been attempted to partially replace the poisonous Pb in perovskites, which points to the new direction in possibly alleviating the toxicity in this field. Mn doping in high band gap semiconductor hosts, where the excitation energy is transferred to a Mn d-state, results in short-range tunable yellow-orange d−d emission. Due to the fact that $Mn^{2+}$ could effectively modulate the electronic and optical properties of II-VI semiconductor nanocrystals [25-26], by using a modified synthetic method with a complicated purification process, the introduction of $Mn^{2+}$ creates electronic states in the midgap region of $CsPbCl_3$ with distinct charge transfer dynamics [27, 28, 29]. Since doping-Mn does not only affect the band gap of the host perovskite, but also the morphology of the films, research [30] suggests that $CsPb_{0.995}Mn_{0.005}I_{1.01}Br_{1.99}$ demonstrates superior quality and homogeneous thickness with high reproducibility. The higher PCE reaches 7.36%, compared with 6.14% of $CsPbIBr_2$, with long lasting operating time of more than 300 h in ambient atmosphere. However, to our best knowledge, there has been no report on the complete substitution of Mn for Pb and the toxicity issue has been not totally addressed by Mn.

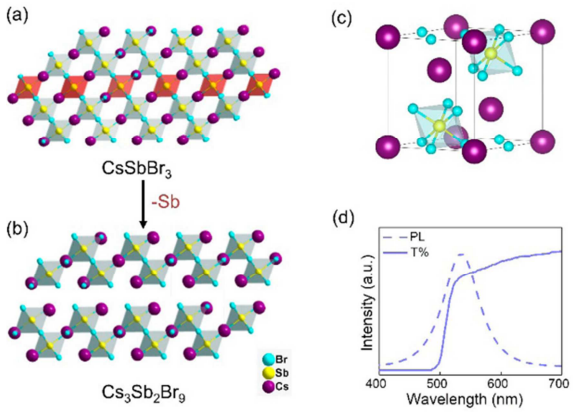


***Figure 3.*** *Schematic illustration of the transformation between the Perovskite Crystal Structures of $CsSbBr_3$ and 2-D layered $Cs_3Sb_2Br_9$ by removing every third Sb layer along the ⟨111⟩ direction in (a) and (b). (c) unit cell of $Cs_3Sb_2Br_9$, (d) Transmission and Photoluminescence spectra of $Cs_3Sb_2Br_9$. Adapted with permission [31]. Copyright 2017, American Chemical Society.*

These considerations raise questions: are there other options to replace Pb in perovskite solar cells by nontoxic elements, without compromising efficiency or stability? Or is Pb absolutely essential? How about the other metal cations with lone-pair s orbitals such as $Bi^{3+}$, $Sb^{3+}$? Due to tri-valence of $Bi^{3+}$, $Sb^{3+}$, in order to enable these heterovalent substitution, the chemical composition needs to be altered as $A_3^+B_2^{3+}X_9^-$, accordingly. Meanwhile, the compounds with formula of $A_3^+B_2^{3+}X_9^-$ can be thought as the same category as "vacancy-ordered" perovskites of $AB_{2/3}X_3$, where one in three octahedral $B^{3+}$ sites is vacant in order to maintain the charge neutrality. More specifically, each vacancy layer and two B-atom layers are alternatively stacked along the <111> direction of the cubic perovskite structure. The structures of them are termed "two dimensional layered perovskite derivatives" and crystallized in P3m1 space group [31], as sketched in Figure 3(a) and (b) about how the structure changes from $CsSbBr_3$ to $Cs_3Sb_2Br_9$. In these compounds, A is a monovalent cation like $Cs^+$or $Rb^+$ and B is a trivalent metal cation like $Bi^{3+}$or $Sb^{3+}$to replace $Pb^{2+}$. The unit cell structure is depicted in Figure 3(c). All these compounds have band gaps around 2.1 eV (For instance, the bandgap of $Cs_3Sb_2I_9$ is 2.05 eV as shown in Figure 3(d) while that of $Cs_3Bi_2I_9$ is even larger of 2.86 eV), poor carrier transport and optical properties. At the same time, the layered perovskites possess reduced band dispersion near the bandgap, resulting in larger effective masses of electrons and holes (0.44-0.62 and 0.60-0.68 $m_0$, respectively). Relatively large bandgap, inferior carrier transport, optical properties, and heavier effective carrier masses are all highly detrimental to the photovoltaic performance. In spite of the fact that they demonstrate less toxicity and excellent stability for over 40 days upon continuous exposure to humidity and ambient surroundings in contrast with the lead-based analogues, expectedly, the reported efficiencies of $Cs_3Bi_2I_9$ and $Rb_3Sb_2I_9$ are very poor, 1.09% [32] and 0.66% [33], respectively.

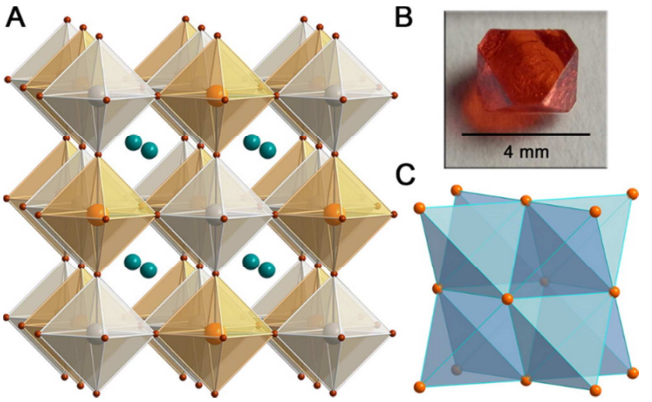


***Figure 4.*** *(A)Schematic illustration of ordered double perovskite crystal structure of $Cs_2AgBiBr_6$. Orange, gray, turquoise, and brown spheres represent Bi, Ag, Cs, and Br atoms, respectively. (B) Photograph of a single crystal of $Cs_2AgBiBr_6$. (C) The $Bi^{3+}$face-centered-cubic sublattice in $Cs_2AgBiBr_6$, consisting of edge-sharing tetrahedra. Reproduced with permission [35]. Copyright 2016, American Chemical Society.*

An alternative possibility to realize lead free compounds while retaining the conventional perovskite structure is to pair B-site with one monovalent and one trivalent metal

cation to form B-Cation-Ordered double perovskite of $A_2B'B''X_6$ with doubled unit cell, in which $B' = Cu^+, Ag^+, Li^+; B'' = Bi^{3+}, Sb^{3+}, Ln^{3+}$. These cations are expected to be able to raise the VBM by forming strong antibonding coupling between cation d/s-anion p orbitals in these new halide double perovskites. Much work remains to be done in order to assess the potential of lead free double halide perovskites, due in part to the seemingly insurmountable difficulty in developing a synthetic route to obtain uniform thin films of the correct phase and composition. According to the available investigations, $Cs_2AgBiBr_6$ is the first halide double perovskite to be considered for photovoltaic applications [34]. The crystal structure of $Cs_2AgBiBr_6$ is sketched in Figure 4. Irrespective of good stability against air and moisture, theoretical calculations suggest that the VBM mainly consists of Ag d-Br 5p antibonding states, while the CMB results from Bi 6p-Br 4p antibonding states, which does not match 3D connectivity, leading to a lower-than-3 electronic dimensionality. Consequentially, an indirect band gap of 1.95 eV is exhibited by $Cs_2AgBiBr_6$ with long carrier recombination life time (660 ns) [35] and highly anisotropic carrier transport properties. Meanwhile, further investigations reveal that the dominant defects, such as Bi vacancy and Ag-on-Bi antisite, create deep states in the bandgap [36], explaining why $Cs_2AgBiBr_6$ cannot be a promising photovoltaic absorber comparable to the Pb-based perovskites. $Cs_2AgInCl_6$ has been reported as a direct-bandgap halide double perovskite. The synthesized $Cs_2AgInCl_6$ displays white coloration with an experimentally measured optical bandgap of 3.3 eV [37], unsuitable for efficient thin-film photovoltaic utilization. As a matter of fact, most of these halide perovskites are highly ionic and have indirect bandgaps, spanning from 1.8-2.2 eV ($Cs_2AgBiBr_6$) to 2.2 eV-2.8eV ($Cs_2AgBiCl_6$) [38-39], which is too large for single-junction solar cells.

### *2.3. Options on X*

So far it has been a widely known fact that X is limited to halide in this newly emerging perovskite solar cell. Single halide on the X site has been attempted, demonstrating advantages and deficiencies. For instance, the stabilized $CsPbBr_3$ with bandgap of 2.3 eV does not absorb light beyond 540 nm [40, 41], greatly limiting its absorption with the best PCE of 10% [42] to date, while $CsPbI_3$ with an appropriate bandgap of 1.73 eV and the to-date PCE of 15.7% [43], however, suffers phase instability [44, 45, 46], with the photoactive α-phase (black) quickly degrading to a non-perovskite δ-phase (yellow) at room temperature and under trace amounts of moisture [47]. Partially replacing the bulky $I^-$ ion with the relatively smaller $Br^-$ ion should stabilize the structure. For instance, the dual halide perovskite ($CsPbI_2Br$) with an increased Goldschmidt tolerance factor (0.84) [48] enables the synthesis $CsPb(Br_xI_{1-x})_3$ perovskites to be thermodynamically more favorable at room temperature [49]. More significantly, controlling the halide stoichiometry in $CsPbX_3$ has been explored as an effective means for tuning the bandgap. For example, from iodine-rich to bromine-rich phases, the bandgaps of $CsPbI_2Br$ and $CsPbIBr_2$ are 1.91 eV and 2.05 eV, respectively. Among all the dual halide all-inorganic perovskites, $CsPbI_2Br$ turns out to be the most studied mixed halide not only because of its narrower bandgap, but also due to a much improved ambient stability. The device fabricated with $CsPbIBr_2$ has a PCE of 6.3% with a spray-assisted solution process [50-51], which allows for a sequential solution process of $CsPbIBr_2$, overcoming the solubility issue of bromide ion in the precursor solution that would otherwise occur in one step solution process. However, in air an optimal annealing temperature of 300°C is required which plays a critical role in the film quality and device performance, because the higher temperature could result in excess CsI in the film. The hole-transport-layer free $CsPbIBr_2$ based solar cells deposited by dual source thermal evaporation has shown a PCE of 4.7% with the 12-h stability at 200°C in a nitrogen glovebox and 2-h duration at 150°C in the ambient atmosphere [52]. Owing to the high density of unfavorable defects and mismatched band alignment in the devices, the most studied $CsPbI_2Br$ perovskite solar cells yielded a relatively low open-circuit voltage (<1.2V) and a low short-circuit current density (<14mA/cm$^2$), leading to a poor PCE commonly below 12%. Strategies to control $CsPbI_2Br$ growth (optimizing annealing temperature [53], solvent control growth [43]) for effectively reducing defects allow the PCE to achieve 14.6% [54]. A precursor engineering process could push the PCE to a value of 14.78% [55], while a temperature-assisted crystallization process further increases the PCE to 14.81% [56]. In 2019, Chen and coworkers [57] reported the PCE of 16.07% with robust stability against moisture and oxygen after 120h under 100 mW/cm$^2$ UV irradiation. The synergetic approach they adopted consists of gradient thermal annealing and anti-solvent treatment to attain a high quality $CsPbI_2Br$ film with a low defect density. Amazingly, the device could retain 95% of its initial efficiency for up to 1000 h with 30% humidity at room temperature.

Some efforts have been devoted to reduce toxicity for the mixed halide perovskites, like $CsPb_{0.9}Sn_{0.1}IBr_2$ [58], which was prepared via the facile solution approach under ambient conditions, demonstrating a suitable bandgap of 1.79 eV. When incorporating carbon as counter electrodes, the device fabricated with $CsPb_{0.9}Sn_{0.1}IBr_2$ exhibits a high open-voltage of 1.26 V and an excellent PCE up to 11.33%, breaking the record among the existing Sn-based perovskite solar cells.

## 3. Synthesis Routes for High Efficiency All Inorganic Perovskites Solar Cells

### *3.1. Hot Inject Method*

Hot inject method is widely adopted for the preparation of $CsPbX_3$, particularly in nanocrystal structures. The method to produce $CsPbX_3$ nanotubes, based on high temperature hot injection, was developed by Kovalenko [59] and coworkers

in 2015, and refined by other research groups like Alivisatos [60] and coworkers to synthesize nanoplatelets. According to the hot-injection method for synthesizing conventional semiconductors in quantum dots [61], $Cs_2CO_3$ is added into a mixture of 1-octadecene and oleic acid and then dried at 120 °C for 1 h, followed by being heated to 150°C under $N^2$. The obtained cesium oleate solution is kept at 100°C to prevent precipitation. Next, a mixture of 1-octadecene and $PbX_2$ is vacuum-dried at 120°C for 1 h and purged with $N^2$. Dried oleylamine and dried oleic acid are added to the solution at 120°C. After $PbX_2$ is completely dissolved, the solution is heated to a certain temperature between 140°C and 200°C to finely tune the size of the nanocrystals. The pre-heated solution of cesium oleate is quickly injected into the solution containing $PbX_2$ at the right temperature. 5 s later, the mixture is cooled in an ice-water bath to cause precipitation of $CsPbX_3$ nanocrystals. The nanocrystals are collected by centrifugation, and re-dispersed in toluene or hexane to obtain a stable colloidal solution for film development. The experimental setup for hot injection is shown in Figure 5. This tedious hot injection method demands high temperature, is generally performed under an inert atmosphere, and only can be applied to control the thickness of bromine-based perovskites [62]. Later on, Seth et al [63] reported an injection synthesis route at room temperature, in an open atmosphere, which is facile and highly reproducible, yielding up to 6 different morphologies by varying the solvent, ligand and reaction time.

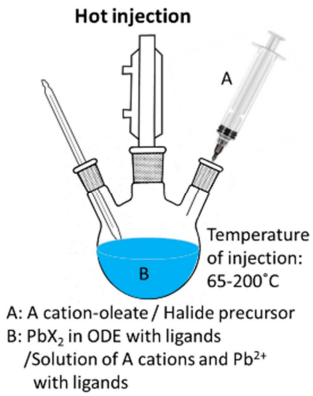


***Figure 5.*** *Diagram for hot-injection synthesis approach. Reproduced with permission [61]. Copyright 2015, American Chemical Society.*

### *3.2. Most Popular Solution Approach*

To deposit all-inorganic perovskites on a substrate, the most adopted, cost-effective, ease methods are one-step or two-step coating method [64-65], which are illuminated in Figure 6. The appropriately mixed CsI and $PbI_2$ solution is spin-coated (for one-step) to form all inorganic perovskite thin films in which the solute of CsI and $PbI_2$ are dissolved in the proper solvent, commonly used, a polar aprotic one like N, N-dimethylformamide (DMF), dimethyl sulfoxide (DMSO), or gamma-butyrolactone (GBL) as a coating solution. Drying and annealing are required after coating. The two-step approach is to spin coat CsI solution after coating with $PbI_2$. After $PbI_2$ film is formed on a substrate, the solution of CsI is spun on the $PbI_2$ film. In order to obtain high quality perovskite films, it is of vital importance to optimize the coating parameters such as spinning speed, time, temperature, solution wettability and viscosity, etc. It turns out that quality perovskite films with better morphology and interfaces could be attained by the two-step method, which is also reflected by the better PV performance solar cells.

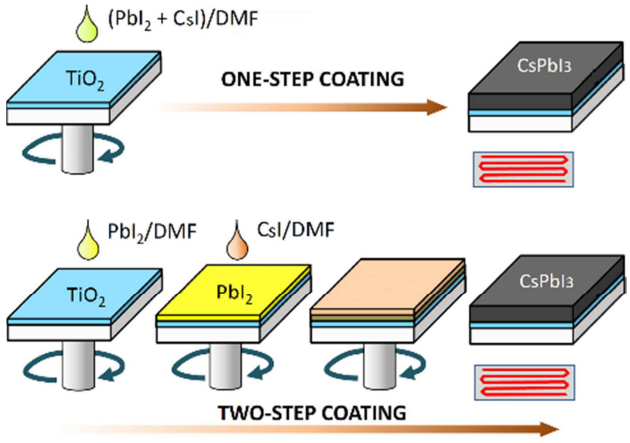


***Figure 6.*** *Schematic diagrams for one-step and two-step synthesis approaches. Adapted with permission [65]. Copyright 2014, American Institute Physics LLC.*

### *3.3. Vapor Assisted Solution Approach/Spray Assisted Solution Approach*

Apparently, the morphology control of perovskite film plays a crucial role in achieving high efficiency perovskite solar cells because numerous devices suffer from short-circuiting issues without any efficiencies due to the poor quality of films. Although the solution approach is facile, not energy-intensive, and ready for mass production, the undesired pinholes in the film could not be effectively avoided, leading to non-continuous perovskite film in which shunting pathways are introduced, hampering the solar cell performance. The formation of pinholes is attributed to the lack of ideal solvents that can simultaneously dissolve several components. Another limitation of the solution approach is that incomplete surface coverage sometimes occurs, which deteriorates the film quality and limits the device performance. In order to remedy the situation, vapor/spray assisted solution approach [66] can serve as an alternative method. As indicated in the figure, the vapor/spray-assisted solution approach is as follows: a) pre prepare the substrate; b) develop inorganic precursor solution into film onto the pre-prepared substrate by spin-coating; c) subsequently treat with the proper inorganic vapor/spray (this step can be repeated a couple of times); d) perovskite film will be developed via in situ reaction. This approach takes advantage of the high kinetic reactivity of vapor and thermodynamic stability of perovskite during the in situ growth to ensure quality film with well-defined grain

structure and even up to microscale grain sizes, along with full surface coverage. Meantime, co-deposition of inorganic solutions is avoided so that the formation of pinholes is prevented [67]. Similarly, a spray-assisted solution process, as good as the vapor one, can yield a well-defined grain structure with grain sizes up to the microscale, full surface coverage, and small surface roughness [1, 50, 68, 50]. The detailed steps are indicated in Figure 7, in which the quality films with reduced pinholes are attained by the spray-assisted solution approach after repeating the spray several times.

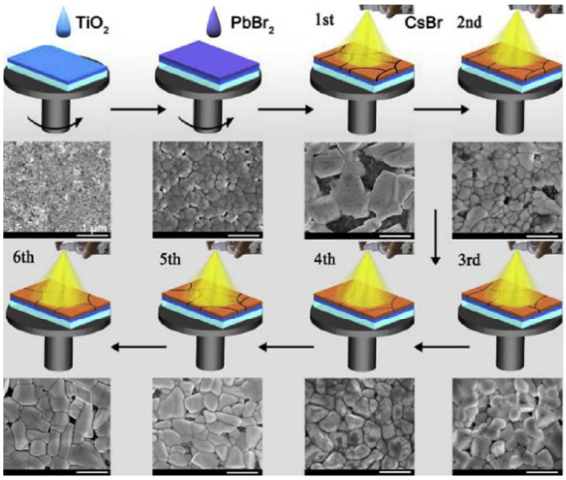


***Figure 7.*** *Illustrated diagrams for spray-assisted solution approach to synthesize quality film of $CsPbBr_3$. Reproduced with permission [68]. Copyright 2018, Elsevier Publishing.*

### *3.4. Thermal Evaporation/Vacuum Process*

For the preparation for all inorganic perovskite films, the thermal/vacuum evaporation approach is rarely adopted due to the fussy and complicated process. For the purpose of review, the details about this process are introduced. The dual source evaporation system [52, 69, 70] with ceramic crucibles is installed as illustrated in Figure 8, CsI and $PbI_2$ can be co-evaporated from separate crucibles at $10^{-5}$ mbar with an as-deposited molar ratio 1:1. The dark brown color appears right after evaporation. Annealing is needed to crystallize the as-deposited perovskite. For the thin perovskite films, co-evaporation is required under the pressure of $10^{-6}$ mbar, the crucible with CsI is heated to 70°C and the other with $PbI_2$ is heated to 250°C. Very recently, Ajjouri et al [71] have reported that inorganic halide perovskite is deposited by using a single source. It seems that the thermal evaporation approach could more effectively control the thickness of the films when compared with the solution method. However, since thermal evaporation requires high vacuums and sophisticated equipment, it restricts cost effectiveness and mass production.

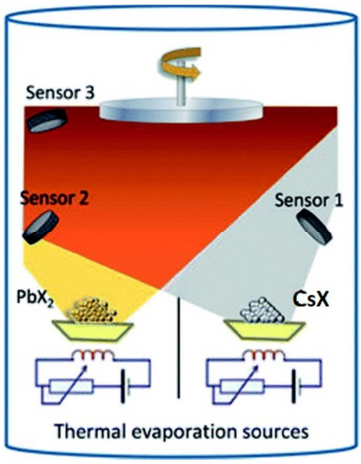


***Figure 8.*** *Schematic illustration for Thermal evaporation approach for synthesis $CsPbX_3$. Adapted with permission [70]. Copyright 2015, Materials Research Society.*

### *3.5. Ultra-Sonication Method*

Interestingly, Tong et al [72] reported that $CsPbX_3$ can be prepared with tunable composition and thickness by using an Ultra-sonication method, as shown in Figure 9(a). X can be replaced by Cl, Br or I as indicated in Figure 9(b). Mixtures of precursor salts ($Cs_2CO_3$ and $PbX_2$) and capping ligands (Oleylamine and oleic acid) in a nonpolar solvent (mineral oil or octadecent) are directly sonicicated with a sonication tip under ambient conditions. This facile and ease route is followed by a sonication process to prepare for metal nanoparticles due to metal-ligand complex formation under ultra-sonication. The required device is merely an ultra-sonicator.

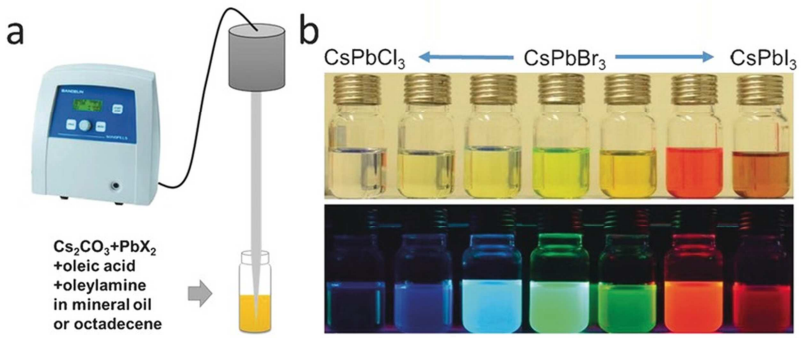


***Figure 9.*** *Schematic diagram for Ultra sonication approach for $CsPbX_3$ and Various products. Reproduced with permission [72]. Copyright 2016, WILEY-VCH Verlag GmbH & Co. KGaA.*

### *3.6. Microwave Irradiation Method*

Liu et al [73] developed one-step microwave irradiation method in which cesium acetate (CsOAc) and lead halide ($PbX_2$) are mixed in a 50 mL beaker with 1-octadecence (ODE), bis(2,4,4-trimethylpentyl) phosphinic acid (TMPPA) and oleylamine (OLA), then the beaker is put in a microwave oven and heated for a specific time depending on the species of $PbX_2$ (X=Cl, Br and I). They claimed that this single-step microwave-assisted approach is versatile and polar-solvent-free, exhibiting flexibility and simplicity in composition control. Pan et al [74] reported a fast and efficient microwave-assisted strategy for the synthesis of high-quality $CsPbX_3$ NCs with controllable morphologies (nanocube, nanoplate and nanorod) with a high photoluminescence quantum yield at about 75%.

## 4. Variety of Device Structures

The beauty of perovskite solar cells is the diversity in their device architectures due to the distinct material properties, such as, direct band gap ranging from semiconducting to metallic, which is tunable through the choice of the "right ingredients" [75]; broad absorption spectra range with high extinction coefficient; ambipolar diffusion and long carrier diffusion length [76, 77]. They can act as either n-type, p-type, or even intrinsic (i-type) semiconductor, therefore, they could play a dual role as a light absorber and charge transporter. As far as the device architecture is concerned, there are two branches in developing perovskite solar cells: Meso-structure and planar heterojunction as portrayed in Figure 10 (a), (b) &(c).

### *4.1. Meso-structure*

Meso-structure easily traces back to its evolutionary technological ancestry, which are solid state dye-sensitized solar cells. The mesoporous devices are predicated on metallic or insulator oxide (commonly, $TiO_2$ or $ZnO_2$, or with $Al_2O_3$) thick films as scaffolds infiltrated with a perovskite material. Since meso-structures typically require a high temperature sintering step, plastics with low melting points are excluded as support materials. Usually, perovskite solar cells with such configuration consist of a highly crystalline perovskite absorber, a meso-porous electron-transporting layer (ETL) and a hole-transporting layer (HTL), sandwiched between a transparent conducting substrate (TCO) and a metal contact as portrayed in the diagram. In order to avoid shunting losses, a thin compact layer of $TiO_2$ is deposited on TCO. When a mesoporous scaffold layer of inert $Al_2O_3$ is added, this structure is known as a mesoporous super-structured solar cell, in which the insulating scaffold layer helps in the formation of pin-hole free film and induces n-type properties in the scaffold underlying material [78]. The certified PCE of the mesostructured solar cells with about 200 nm of perovskite layer reached above 16% [79]. The mesoporous scaffold structure greatly facilitates the nucleation and growth of perovskites and avoids the formation of pinholes to suppress internal device shunting. In addition, the mesoporous $TiO_2$ scaffold seems to have an effect in suppressing the hysteresis behavior that is generally more severe in the planar structure, evidenced by the initial better efficiency [80]. However, the mesoporous scaffold devices are not easy to commercialize due to the requirements for thermal processing at high temperatures.

### *4.2. Planar Heterojunctions*

The second direction is the solid thin film perovskite solar cells, mostly in the form of n-i-p (or inverted p-i-n, even p-n) planar heterojunctions, which are intensively employed because of the simple device configuration. One advantage over meso-structure is that planar heterojunctions could reduce production costs and difficulties caused by the fabrication of mesoporous layers. More importantly, the removal of the mesoscopic layer considerably simplifies the device fabrication process, often at low temperatures [81], which holds great potential for mass production [82]. In n-i-p heterojunctions, solid perovskites absorber films act as an intrinsic semiconductor (a major light absorbing layer), sandwiched by n-type (mainly as ETL) and p-type (mainly as HTL) materials. While in the inverted p-i-n structure, the hole-selective layer is directly deposited onto TCO substrates and an electron transporting layer on top of the perovskite absorber as depicted in the diagram. In the planar structure, the charge diffusion length of perovskites can be larger than the depth of the light (the film thickness), guaranteeing a higher internal quantum efficiency [83]. Charge carrier mobility (in excess of 20 $cm^2 V^{-1}s^{-1}$) and emissivity in the planar perovskite films are better than those in meso-structured perovskites [78]. Depletion regions at the p-i and i-n are added up and an internal field is established across the entire i-layer, which provides the driving force for separating photo-generated charge carriers. As a result, an open circuit voltage ($V_{OC}$) and a short circuit current ($I_{SC}$) are generated, which decisively determines the photovoltaic performance. Not only could appropriate p-type and n-type materials facilitate the separation of carriers, but they could also enhance light harvesting because absorption at wavelength regions relevant to each material grew as layers were deposited. The record holder PSC adopts the planar architectures. However, the planar device would likely have structural imperfections, such as pinholes, non-homogenous crystal growth, and low coverage associated with planar thin films [84]. Low coverage and non-uniform crystalline network may result in low resistance shunting paths, reducing the maximum attainable open circuit voltage and fill factor, while the poor surface coverage causes the incident photons to pass straight through the uncovered areas, decreasing the available photocurrent. Also excess shunt paths due to direct contact between HTL and ETL lead to the formation of parallel diodes in the solar cell equivalent circuit [85].

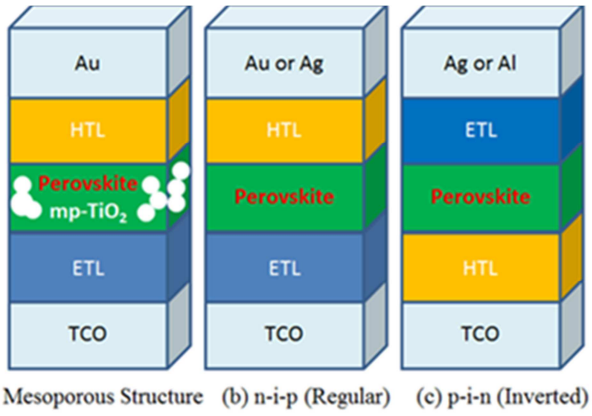


***Figure 10.*** *Illustrated diagrams for various architecture of perovskite solar cells. a) mesoporous structure b) n-i-p structure c) inverted p-i-n configuration.*

Perovskite solar cells could adopt various configurations and each of them have achieved successes. Thus many unanswered questions remain including: 1) Are there significant differences in the working principles among various configurations? 2) What are the physical electronic mechanisms that govern carrier separation, transport, extraction, and their recombination? The answers to those questions are highly mandatory to assess the properties of materials in each layer, electrode contacts, and the overall architecture of the device. Since the perovskite layer not only acts as a photo-absorber to generate carriers, but also transport holes or electrons efficiently to the corresponding electrode directly, the presence of p-layer (HTL) or n-layer (ETL) is not a prerequisite for the device function. In addition, the simpler planar structure will facilitate to better understand the bolts and nuts of perovskite solar devices. Therefore, ETL free [86-88] or HTL free [89-91] devices have been extensively explored, helping thoroughly scrutinize two key interfaces — the perovskite/ETL and the perovskite/HTL since they play vital parts in carrier separation, carrier diffusion and charge transporting. Comparison of the merits of each architecture (p-i-n, p-n without HTL and p-n without ETL) would shed light on the origins of various photovoltaic properties including intense light absorption, long carrier diffusion length, and carrier transport, etc. To date, the simplest device was reported by Duan et al [92] that was built as (FTO)/$CsPbBr_3$ /carbon architecture by a multistep solution-processed deposition technology, achieving an efficiency as high as 4.1% and enhanced stability upon interfacial modification by graphene quantum dots and $CsPbBrI_2$ quantum dots. The concomitant advantage of these simplest solar cells is the riddance of the high cost of a state-of-the-art hole-transporting layer.

## 5. Future Direction and Challenges

All inorganic perovskites, particularly lead free, are of vital significance on both scientific and industrial engineering fronts due to their exceptionally low cost process and meritorious optoelectronic properties promising for widespread applications, not limited to photovoltaic fields. In spite of an inviting vista of commercialization demonstrated by these newly emerging photovoltaic materials, many challenges still lie ahead. At present, lead with an intrinsic superiority seems to be irreplaceable since the performance of lead-free perovskites solar cells has not surpassed that of lead-based analogues although a lot of attention has turned to the development of environmentally friendly perovskites. The toxicity still remains a big issue which cannot be neglected. Additionally, long term stability has been realized, unfortunately, at the cost of efficiency. Most reported PSCs with relatively long term stability in ambient conditions under full sunlight achieve the lackluster PCE [93]. Thus, overcoming instability without sacrificing the efficiency seems formidable. All-inorganic perovskites demonstrate relatively long lasting operating time, but lower efficiency, due in large part to their far-from-optimal bandgap. After all, PSCs still fall into the semiconductor-based PV category, in which the band-gap of backbone materials of perovskite plays a decisive role in the PV effect because only photons with energy higher than (or at least equal to) the band gap can be efficiently absorbed, the photons with energy less than the band gap being completely wasted due to the lack of absorption. As a result, the Shockley-Queisser (SQ) limit places an upper bound on an efficiency of 31% for perovskite solar cells based on the theoretical calculation for a single-gap solar cell's maximum thermodynamic efficiency [94]. Even the PCE of the mixed organic-inorganic PSCs, debuted with 3.8% in 2009; 22.1% in 2016 and 23.3% in August 2018 [2]; seems to have reached a plateau, which is far below the SQ limit of 31%. Thus, breakthroughs in the PCE become more imperative, especially for stabilized inorganic perovskites with considerably poor efficiency. A tandem scheme [95] of different bandgap materials to form double-junction or triple-junction is one of possible strategies to overcome the SQ limit, which has been commonly pursued as "full-spectrum" solar cells to optimally harvest photons [96]. High efficiencies exceeding 30% are predicted for both two terminal and four-terminal configurations with Si/perovskite tandem cells [97]. Albrecht et al [98] in November 2018 reported that the PCE of perovskite-silicon tandem solar cells has achieved 25.5%, which is the highest published value to date. His team constructed an efficient perovskite/silicon tandem solar cell with a back-side etched with a silicon layer. The perovskite layer was spin-coated onto the smooth front-side of the silicon. The team afterwards applied a polymer light management (LM) foil to the front-side of the device which enables processing of a high-quality perovskite film on a flat surface, while still benefiting from the front-side texture. By comparison, modifying the band gap of single band-gap host materials seems more promising. For instance, introducing an additional energy-level into the forbidden as an added trap-level, is called intermediate band (IB) [99]. Or adding the lanthanide series elements with up/down conversion capability [100] into the host materials allows for the increased light harvesting by sequential absorption of

photons so that light absorption is extended to a broader wave-length region on the solar spectrum.

## 6. Conclusions

In all, the most recent developments in material sciences of halide all inorganic perovskites were reviewed, with possible alternatives to lead, the synthesis approaches, assessment of various device configurations and their progress in solar cells. Even some all-inorganic but lead-based counterparts were summarized and compared in order to motivate researchers to explore all the potentials. Surveying recent developments toward lead-free all-inorganic perovskite solar cells and the envisioned future directions would offer a roadmap for developing new materials and navigating uncharted territory in solar energy fields. The new materials development and optimization of device structure and related manufacture technologies greatly hinge on the comprehensive understanding of photovoltaic mechanisms. Therefore, the theoretical consensus about the working mechanisms of perovskite solar cells is in dire need, which can guide more rapid strides in the technologies, pursuing more efficient/stable, more environmentally friendly perovskite materials and novel device design.

## Acknowledgements

This work is supported by National Science Foundation (NSF) (grant no.1700339).

## References

[1] A. Kojima, K. Teshima, Y. Shirai and T. Miyasaka “Organometal Halide Perovskites as Visible-Light Sensitizers for Photovoltaic Cells” J. Am. Chem. Soc. 2009, 131 (17): 6050-6051.

[2] “NREL Efficiency Chart”. https://www.nrel.gov/pv/assets/pdfs/pv-efficiency-chart.20190103.pdf.

[3] A. B. Djurisic, F. Z. Liu, H. W. Tam, M. K. Wong, A. Ng, C. Surya, W. Chen and Z. B. He, “Perovskite solar cells-an overview of critical issues”. Progress in Quantum Electronics 53 (2017) 1-37. https://doi.org/10.1016/j.pquantelec.2017.05.002.

[4] T. J. Jacobsson, L. Josef Schwan, M. Ottosson, A. Hagfeldt, and T. Edvinsson, "Determination of Thermal Expansion Coefficients and Locating the Temperature-Induced Phase Transition in Methylammonium Lead Perovskites Using X-ray Diffraction", Inorg. Chem., 2015, 54 (22), 10678–10685.

[5] Goldschmidt LM, Die Gesetze Der Krystallochemie. Naturewissenschaften, 1926, 14 (21), 477-485.

[6] C. Li, K. C. Soh and P. J. Wu, “Formability of ABO3 perovskites”, J. Alloys, Compd. 2004, 372, 40-48.

[7] G. E. Epero, G. M. Paternò, R. J. Sutton, A. Zampetti, A. A. Haghighirad, F. Cacialli and H. J. Snaith, "Inorganic caesium lead iodide perovskite solar cells", J. Mater. Chem. A 3, 2015, 19588-19695.

[8] W. Ahmad, J. Khan, G. D. Niu and J. Tang, "Inorganic CsPbI3 Perovskite-Based Solar Cells: A Choice for a Tandem Device", J. Solar RRL, 2017, 1, 1700048.

[9] Y. H. Hu, M. F. AygÜler, M. L. Petrus, T. Bein and P. Dpcampo, “impact of Rubidium and Cesium cations on the moisture stability of multiplie-cation mixed halide perovskites”, ACS Energy Lett. 2017, 2, 2212-2218.

[10] T. Duong, H. K. Mulmudi, H. Shen, Y. Wu, C. Barugkin, Y. O. Mayon, H. T. Nguyen, D. Macdonald, J. Peng, M. Lockery, et al.”structural engineering using Rubidium Iodide as a dopant under excess lead iodide conditions for high efficiency and stable perovskites”, Nano Energy 2016, 30, 330-340.

[11] Z. Liu, T. Zhang, Y. F. Wang, C. Y. Wang, P. Zhang, H. Sarvari, Z. Chen and S. B. Li, “Electronic properties of a new all-inorganic perovskite TlPbI3 simulated by the first principles”, Nanoscale Research Letters, 2017 (12) 232.

[12] F. Giustino, and H. J. Snaith, "Toward Lead-Free Perovskite Solar Cells”, ACS Energy Lett. 2016, 1, 1233−1240, DOI: 10.1021/acsenergylett.6b00499.

[13] A. Y. Mei, X. Li, L. F. Liu, Z. L. Ku, T. F. Liu, Y. G. Rng, M. Xu, M. hu, J. Z. Chen, Y. Yang, M. Grätzel and H. W. Han, “A hole-conductor-free, fully printable mesoscopic perovskite solar cell with high stability”, Science, 2014, 345, 295-297.

[14] A. B. Djurisic, F. Z. Liu, H. W. Tam, M. K. Wong, A. Ng, C. Surya, W. Chen and Z. B. He, “Perovskite solar cells-an overview of critical issues”. Progress in Quantum Electronics 53 (2017) 1-37. https://doi.org/10.1016/j.pquantelec.2017.05.002.

[15] Z. W. Xiao and Y. F. Yan, “progress in theoretical study of metal halide perovskite solar cells materials”, Adv. Energy. Mater. 2017, 7, 1701136.

[16] C. C. Stoumpos, C. D. Malliakas and M. G. Kanatzidis, "Semiconducting tin and lead iodide perovskites with organic cations: phase transitions, high mobilities, and near-infrared photoluminescent properties." Inorg. Chem. 2013, 52 (15): 9019-38. Doi: 10.1021/ic401215x.

[17] M. H. Kumar, S. Dharani, W. L. Leong, P. P. Boix, R. R. Prabhakar, T. Baikie, C. Shi, H. Ding, R. Ramesh, Asta, M. Gratzel, S. G. Mahaisalkar and N. Mathews. “lead-free halide perovskite solar cells with high photocurrents realized through vacancy modulation”, Adv. Mater. 2014, (26) 7122-7127.

[18] D. Sabba, H. K. Mulmudi, R. R. Prabhakar, T. Krishnamoorthy, T. Baikie, P. P. Boix, S. G. Mahaisalkar and N. Mathews, “impact of anionic Br-substitution on open circuit voltage in lead free perovskite (CsSnI3-xBrx)solar cells” J. Phys. Chem. C 2015, 119, 1763-1767.

[19] K. P. Marshall, M. Walker, R. I. Walton and R. A. Hatton, "Enhanced stability and efficiency in hole-transport-layer-free CsSnI3 perovskite photovoltaics", Nature Energy, 2016 Vol. 1, Article number: 16178.

[20] W. J. Ke, C. C. Stoumpos, M. H. Zhu, L. L. Mao, I. Spanopoulos, J. Liu, O. Y. Kontsevoi, M. Chen, D. Sarma, Y. B. Zhang, M. R. Wasielewski and M. G. Kanatzidis1, "Enhanced photovoltaic performance and stability with a new type of hollow 3D perovskite FASnI3", Science Advances, 2017, Vol. 3, no. 8, e1701293, DOI: 10.1126/sciadv.1701293.

[21] L. Zhou, J.-F. Liao, Z.-G. Huang, X.-D. Wang, Y.-F. Xu, H.-Y. Chen, D.-B. Kuang, and C.-Y. Su, "All-Inorganic Lead-Free Cs2PdX6 (X = Br, I) Perovskite Nanocrystals with Single Unit Cell Thickness and High Stability", ACS Energy Lett., 2018, 3 (10), 2613–2619.

[22] A. Kaltzoglou, M. Antoniadou, A. G. Kontos, K. Stoumpos, D. Perganti, E. Siranidi, V. Raptis, K. Trohidou, V. Psycharis, M. Kanatzidis and P. Falaras, "Optical-Vibrational Properties of the Cs2SnX6 (X = Cl, Br, I) Defect Perovskites and Hole-Transport Efficiency in Dye-Sensitized Solar Cells", J. Phys. Chem. C. 2016, 120, 11777-11785.

[23] W. Ming, H. Shi and M. H. Du, "Large dielectric constant, high acceptor density, and deep electron traps in perovskite solar cell material CsGeI3", J. Mater. Chem. A. 2016, 4, 13852.

[24] F. Yang, D. Hirotani, G. Kapil, M. A. Kamarudin, C. H. Ng, Y. H. Zhang, Q. Shen and S. Z. Hayase, "all-inorgaic CsPbGeI2Br perovskite with enhanced phase stability and photovoltaic performance", Angew. Chem. Int. Ed., 2018, 57, 12745-12749.

[25] A. Nag, R. Cherian, P. Mahadevan, A. V. Gopal, A. Hazarika, A. Mohan, A. S. Vengulekar, D. D. Sarma, "Size-Dependent Tuning of Mn2+ d Emission in Mn2+-Doped CdS Nanocrystals: Bulk vs Surface", J. Phys. Chem. C, 2010, 114, 18323.

[26] N. S. Karan, D. D. Sarma, R. M. Kadam, N. Pradhan, "Doping Transition Metal (Mn or Cu) Ions in Semiconductor Nanocrystals", J. Phys. Chem. Lett. 2010, 1, 2863.

[27] A. K. Guria, S. K. Dutta, S. Das Adhikari, N. Pradhan, "Doping Mn2+ in Lead Halide Perovskite Nanocrystals: Successes and Challenges", ACS Energy Lett. 2017, 2, 1014.

[28] W. J. Mir, M. Jagadeeswararao, S. Das, A. Nag, "Colloidal Mn-Doped Cesium Lead Halide Perovskite Nanoplatelets" ACS Energy Lett. 2017, 2, 537.

[29] W. Y. Liu, Q. L. Lin, H. B. Li, K. F. Wu, I. Robel, J. M. Pietryga, V. I. Klimov, "Mn2+-Doped Lead Halide Perovskite Nanocrystals with Dual-Color Emission Controlled by Halide Content", J. Am, Chem. Soc. 2016, 138, 14954.

[30] J. Liang, Z. H. Liu, L. B. Qiu, Z. Hawash, L. Q. Meng, Z. F. Wu, Y. Jiang, L. K. Ono and Y. B. Qi, "Enhancing optical, electronic, crystalline and morphological properties of Cesium lead halide by Mn substitution for high-stability all-inorganic perovskite solar cells with carbon electrodes", Adv. Energy Mater. 2018, 8, 1800504-1800511.

[31] J. Zhang, Y. Yang, H. Deng, U. Farooq, X. k. Yang, J. Khan, J. Tang, and H. S. Song, "High Quantum Yield Blue Emission from Lead-Free Inorganic Antimony Halide Perovskite Colloidal Quantum Dots". ACS Nano, 2017, 11 (9), pp 9294–9302.

[32] B.-W. Park, B. Philippe, X. L. Zhang, H. Rensmo, G. Boschloo and E. M. J. Johansson, "Bismuth Based Hybrid Perovskites A3Bi2I9 (A: Methylammonium or Cesium) for Solar Cell Application". Adv. Mater., 2015, Vol. 27 (43), 6806-6813.

[33] P. C. Harikesh, H. K. Mulmudi, B. Ghosh, T. W. Goh, Y. T. Teng, K. Thirumal, M. Lockrey, K. Weber, T. M. Koh, S. Z. Li, S. Mhaisalkar, and N. Mathew, "Rb as an Alternative Cation for Templating Inorganic Lead-Free Perovskites for Solution Processed Photovoltaics", Chem. Mater., 2016, 28 (20), 7496–7504.

[34] C. C. Wu, Q. H. Zhang, Y. Liu, W. Luo, X. Guo, Z. R. Huang, H. K. Ting, W. H. Sun, X. R. Zhong, S. Y. Wei, S. F. Wang, "The Dawn of Lead-Free Perovskite Solar Cell: Highly Stable Double Perovskite Cs2AgBiBr6 Film", Adv Sci (Weinh). 2018, 5 (3), 1700759.

[35] A. H. Slavney, T Hu, A. M. Lindenberg, and H. I. Karunadasa, "A Bismuth-Halide Double Perovskite with Long Carrier Recombination Lifetime for Photovoltaic Applications", J. Am. Chem. Soc., 2016, 138 (7), 2138–2141.

[36] Z. W. Xiao, W. W. Meng, J. B. Wang and Y. F. Yan, "Thermodynamic Stability and Defect Chemistry of Bismuth-Based Lead-Free Double Perovskites" Chemsus Chem., 2016, Vol. 9 (18), 2628-2633. Special Issue: Stability of Perovskite Solar Cells & Devices.

[37] G. Volonakis, A. A. Haghighirad, R. L. Milot, W. H. Sio, M. R. Filip, B. Wenger, M. B. Johnston, L. M. Herz, H. J. Snaith and F. Giustino, "Cs2InAgCl6: A New Lead-Free Halide Double Perovskite with Direct Band Gap", J. Phys. Chem. Lett., 2017, 8 (4), 772–778.

[38] G. Volonakis, M. R. Filip, A. A. Haghighirad, N. Sakai, B. Wenger, H. J. Snaith and F Giustino, "Lead-Free Halide Double Perovskites via Heterovalent Substitution of Noble Metals", J. Phys. Chem. Lett., 2016, 7 (7), 1254–1259.

[39] M. R. Filip, S. Hillman, A. A. Haghighirad, H. J. Snaith and F. Giustino, "Band Gaps of the Lead-Free Halide Double Perovskites Cs2BiAgCl6 and Cs2BiAgBr6 from Theory and Experiment", J. Phys. Chem. Lett., 2016, 7 (13), 2579–2585.

[40] X. S. Zhang, Z. W. Jin, J. R. Zhang, D. L. Bai, H. Bian, K. Wang, J. Sun, Q. Wang, and S. Z. F. Liu, "All-Ambient Processed Binary CsPbBr3–CsPb2Br5 Perovskites with Synergistic Enhancement for High-Efficiency Cs–Pb–Br-Based Solar Cells", ACS Appl. Mater. Interfaces 2018, 10, 8, 7145-7154.

[41] Q. A. Akkerman, M. Gandini, F. D. Stasio, P. Rastogi, F. Palazon, G. Bertoni, J. M. Ball, M. Prato, A. Petrozza & L. Manna, "Strongly emissive perovskite nanocrystal inks for high-voltage solar cells", Nature Energy, 2016, vol. 2, Article number: 16194.

[42] J. L. Duan, Y. Y. Zhao, B. L. He and Q. W. Tang, "High-Purity Inorganic Perovskite Films for Solar Cells with 9.72 % Efficiency", Angew. Chem. Int. Ed. 2018, 130, 3849-3853.

[43] P. Y. Wang, X. W. Zhang, Y. Q. Zhou, Q. Jiang, Q. F. Ye, Z. M. Chu, X. X. Li, X. L. Yang, Z. G. Yin & J. B. You, "Solvent-controlled growth of inorganic perovskite films in dry environment for efficient and stable solar cells", Nature Communications, 2018, vol. 9, Article number: 2225.

[44] A. Swarnkar, A. R. Marshall1, E. M. Sanehira, B. D. Chernomordik, D. T. Moore, J. A. Christians, T. Chakrabarti, J. M. Luther, "Quantum dot–induced phase stabilization of α-CsPbI3 perovskite for high-efficiency photovoltaics", Science, 2016, Vol. 354, Issue 6308, 92-95, DOI: 10.1126/science.aag2700.

[45] T. Y. Zhang, M. I. Dar, G. Li, F. Xu, N. J. Guo, M. Grätzel and Y. X. Zhao, "Bication lead iodide 2D perovskite component to stabilize inorganic α-CsPbI3 perovskite phase for high-efficiency solar cells", Science Advances 2017, Vol. 3, no. 9, e1700841, DOI: 10.1126/sciadv.1700841.

[46] B. Li, Y. N. Zhang, L. Fu, T. Yu, S. J. Zhou, L. Y. Zhang & L. W. Yin, "Surface passivation engineering strategy to fully-inorganic cubic CsPbI3 perovskites for high-performance solar cells", Nature Communications, 2018 vol. 9, Article number: 1076.

[47] R. J. Sutton, G. E. Eperon, L. Miranda, E. S. Parrott, B. A. Kamino, J. B. Patel, M. T. Hörantner, M. B. Johnston, A. A. Haghighirad, D, T. Moore and H. J. Snaith, "Bandgap-Tunable Cesium Lead Halide Perovskites with High Thermal Stability for Efficient Solar Cells", Adv. Energy Mater. 2016, Vol. 6, Issue 8, 1502458.

[48] Z. Zeng, J. Zhang, X. Gan, H. Sun, M. Shang, D. Hou, C. Lu, R. Chen, Y. Zhu and L. Han, "in situ grain boundary functionalization for stable and efficient inorganic CsPbI2Br perovskite solar cells", Adv. Energy Mater. 2018, 8, 1801050.

[49] W. J. Yin, Y. Yan and S. H. Wei, "Anomalous alloy properties in mixed halide perovskites." J. Phys. Chem. Lett. 2014, 5, 625-3631.

[50] C.-Y. Chen, H.-Y Lin, K.-M. Chiang, W.-L. Tsai, Y.-C. Huang, C.-S. Tsao and H.-W. Lin, "All-Vacuum-Deposited Stoichiometrically Balanced Inorganic Cesium Lead Halide Perovskite Solar Cells with Stabilized Efficiency Exceeding 11%", 2017, 29, 1605290.

[51] C. F. J. Lau, X. F. Deng, Q. S. Ma, J. H. Zheng, J. S. Yun, M. A. Green, S. J. Huang, and A. W. Y. Ho-Baillie, "CsPbIBr2 Perovskite Solar Cell by Spray-Assisted Deposition", ACS Energy Lett., 2016, 1 (3), 573–577.

[52] Q. S. Ma, S. J. Huang, X. M. Wen, M. A. Green and A. W. Y. Ho-Baillie, "Hole Transport Layer Free Inorganic CsPbIBr2 Perovskite Solar Cell by Dual Source Thermal Evaporation", Adv. Energy Mater. 2016, Vol. 6, 1502202

[53] J. K. Nam, M. S. Jung, S. U. Chai, Y. J. Choi, D. H. Kim and J. H. Park, "Unveiling the Crystal Formation of Cesium Lead Mixed-Halide Perovskites for Efficient and Stable Solar Cells" J. Phys. Chem. Lett. 2017, 8, 2936-2940.

[54] L. Yan, Q. F. Xue, M. Y. Liu, Z. L. Zhu, J. J. Tian, Z. C. Li, Z. Chen, Z. M. Chen, H. Yan, H.-L. Yip and Y. Cao, "Interface Engineering for All-Inorganic CsPbI2Br Perovskite Solar Cells with Efficiency over 14%", Adv. Mater. 2018, 30, 1802509.

[55] G. N. Yin, H. Zhao, H. Jiang, S. H. Yuan, T. Q. Niu, K. Zhao, Z. K. Liu and S. Z. (Frank) Liu, "Precursor Engineering for All-Inorganic CsPbI2Br Perovskite Solar Cells with 14.78% Efficiency", Adv. Funct. Mater. 2018, 28, 1803269.

[56] D. L. Bai, H. Bian, Z. W. Jin, H. R. Wang, L. N. Meng, Q. Wang and S. Z. (Frank) Liu, "Temperature-assisted crystallization for inorganic CsPbI2Br perovskite solar cells to attain high stabilized efficiency 14.81%", Nano. Energy 2018, 52, 408-415.

[57] W. J. Chen, H. Y. Chen, G. Y. Xu, R. M. Xue, S. H. Wang, Y. W. Li and Y. F. Li, "Precise control of crystal growth for highly efficient CsPbI2Br perovskite solar cells", Joule, 2019, 3, 1-14.

[58] J. Liang, P. Y. Zhao, C. X. Wang, Y. R. Wang, Y. Hu, G. Y. Zhu, L. B. Ma, J. Liu and Z. Jin, "CsPb0.9Sn0.1IBr2 Based All-Inorganic Perovskite Solar Cells with Exceptional Efficiency and Stability", J. Am. Chem. Soc., 2017, 139 (40), 14009–14012.

[59] L. Protesescu, S. Yakunin, M. I. Bodnarchuk, F. Krieg, R Caputo, C. H. Hendon, R. X. Yang, A. Walsh and M. V. Kovalenko, "Nanocrystals of Cesium Lead Halide Perovskites (CsPbX3, X = Cl, Br, and I): Novel Optoelectronic Materials Showing Bright Emission with Wide Color Gamut", Nano Lett., 2015, 15 (6), 3692–3696

[60] Y. Bekenstein, B. A. Koscher, S. W. Eaton, P. D. Yang and A. P. Alivisatos, "Highly Luminescent Colloidal Nanoplates of Perovskite Cesium Lead Halide and Their Oriented Assemblies", J. Am. Chem. Soc., 2015, 137 (51), 16008–16011.

[61] F. Zhang, H. Zhong, C. Chen, X. G. Wu, X. Hu, H. Huang, J. Han, B. Zou and Y. Dong, "Brightly Luminescent and Color-Tunable Colloidal CH3NH3PbX3 (X = Br, I, Cl) Quantum Dots: Potential Alternatives for Display Technology." ACS Nano. 2015, 9 (4): 4533-42.

[62] Y. Isoz and T. Isobe, "Review—Synthesis, Luminescent Properties, and Stabilities of Cesium Lead Halide Perovskite Nanocrystals", ECS Journal of Solid State Science and Technology, 2018, 7 (1) 3040-R3045.

[63] S. Seth and A. Samanta, "a facile methodology for engineering the morphology of CsPbX3 perovskite nanocrystals under ambient condition", Scientific Reports, 2016, 6 37693.

[64] H. S. Juang and N. G. Park, "perovskite solar cells: from materials to devices", small, 2015, 11 (1) 10-25.

[65] J.-H. Im, H.-S. Kim, and N.-G. Parka, "Morphology-photovoltaic property correlation in perovskite solar cells: One-step versus two-step deposition of CH3NH3PbI3", APL Mater. 2014, 2, 081510.

[66] W. Zhang, M. Saliba, D. T. Moore, S. K. Pathak, M. T. Hörantner, T. Stergiopoulos, S. D. Stranks, G. E. Eperon, J. A Alexander-Webber, A. Abate, A. Sadhanala, S. H. Yao, Y. L. Chen, R. H. Friend, L. A. Estroff, U. Wiesner and H. J. Snaith, "Ultra-smooth organic–Inorganic perovskite thin-film formation and crystallization for efficient planar heterojunction solar cells," Nature Communication, 2015, article number: 6142. DOI: 10.1038/ncomms7142.

[67] H. P. Zhou, Q. Chen and Y. Yang, "Vapor-assisted solution process for perovskite materials and solar cells", Vol. 40, 2015, 667-673. DOI: 10.1557/mrs.2015.171.

[68] J. L. Duan, D. W. Dou, Y. Y. Zhao, Y. D. Wang, X. Y. Yang, H. W. Yuan, B. L. He and Q. W. Tang, "Spray-assisted deposition of CsPbBr3 films in ambient air for large-area inorganic perovskite solar cells", Material Today Energy, 2018 (10), 146-152.

[69] C. Momblona, L. Gil-Escrig, E. Bandiello, E. M. Hutter, M. Sessolo, K. Lederer, J. Blochwitz-Nimoth and H. J. Bolink, "Efficient vacuum deposited p-i-n and n-i-p perovskite solar cells employing doped charge transport layers", Energy Environ. Sci., 2016, 6, 3456-3463.

[70] M. Sessolo, C. Momblona, L. Gil-Escrig and H. J. Bolink, "Photovoltaic devices employing vacuum-deposited perovskite layers", MRS Bull., 2015, 40, 660-666.

[71] Y. E. Ajjouri, F. Palazon, M. Sessolo and H. J. Bolink, "single source vacuum deposition of mechanosynthesized inorganic halide perovskites", Chem. Mater., 2018, 30 (21), 7423-7427.

[72] Y. Tong, E. Bladt, M. F. Ayguler, A. Manzi, K. Z. Milowska, V. A. Hintermayr, P. Docampo, S. Bals, A. S. Urban, L. Polavarapu and J. Feldmann, "highly luminescent cesium lead halide perovskite perovskite nanocrystals with tunable composition and thickness by Ultrasonication", Angew. Chem. Int. Ed., 2016, 55, 13887-13892.

[73] H. W. Liu, Z. N. Wu, H. Gao, J. R. Shao, H. Y. Zou, D. Yao, Y. Liu, H. Zhang and B. Yang, "One step preparation of Cesium lead halide CsPbX3(X=Cl, Br and I) perovskite nanocrystals by microwave irradiation", ACS Appl. Mater. Inferfaces, 2017, 9, 42919-42927.

[74] Q. Pan, H. C. Hu, Y. T. Zou, M. Chen, L. Z. Wu, D. Yang, X. L. Yuan, J. Fan, B. Q. Sun and Q. Zhang, "Microwave-assisted synthesis of high-quality "all-inorganic" CsPbX3 (X = Cl, Br, I) perovskite nanocrystals and their application in light emitting diodes", J. Mater. Chem. C, 2017, 5, 10947-10954.

[75] J. H. Noh, S. H. Im, J. H. Heo, T. N. Mandal and S. I. Seok "Chemical Management for Colorful, Efficient, and Stable Inorganic–Organic Hybrid Nanostructured Solar Cells" Nano Lett. 2013 (13): 1764.

[76] F. Zuo, S. T. Williams, P.-W. Liang, Ch.-Ch. Chueh, Ch.-Y. Liao, and A. K.-Y. Jen, "Binary-Metal Perovskites toward High-Performance Planar-Heterojunction Hybrid Solar Cells" Adv. Mater. 2014 (26) 6454-6460.

[77] C. Zuo, H. J. Bolink, H. W. Han, J. S. Huang, D. Cahen and L. M. Ding "Advances in Perovskites Solar Cells"Adv. Sci. 2016, 1500324.

[78] T. Leijtens, "electronic properties of meso-superstructured and planar organometal halide perovskite films: charge trapping, photodoping, and carrier mobility". ACS Nano 2014, 8 (7), 7147-7155.

[79] N. J. Jeon, J. H. Noh, Y. C. Kim, W. S. Yang, S. Ryu, S. I. Seok, "Solvent engineering for high-performance inorganic-organic hybrid perovskite solar cells." Nat Mater. 2014 13 (9): 897-903.

[80] J.-P. Correa-Baena, A. Abate, M. Saliba, W. Tress, T. J. Jacobsson and A. Hagfeldta, "The rapid evolution of highly efficient perovskite solar cells", Energy environ. sci. 2017, 10, 710-727.

[81] X. Li, M. I. Dar, C. Y. Yi, J. S. Luo, M. Tschumi, S. M. Zakeeruddin, M. K. Nazeeruddin, H. W. Han and M. Grätzel, "Improved performance and stability of perovskite solar cells by crystal crosslinking with alkylphosphonic acid ω-ammonium chlorides", Nature Chemistry 2015, vol. 7, 703–711.

[82] C. Sun, Q. Xue, Z. Hu, Z. Chen, F. Huang, H.-L. Yip and Y. Cao, "Scalable fabrication of efficient organolead trihalide perovskite solar cells with doctor-bladed active layers" Small, 2015, 11, 3344.

[83] M. Z. Liu, M. B. Johnston and H. J. Snaith, "Efficient planar heterojunction perovskite solar cells by vapour deposition", Nature 2013, vol. 501, 395–398.

[84] F. Zabihi, M-R. Ahmadian-Yazdi and M. Eslamian, "Fundamental Study on the Fabrication of Inverted Planar Perovskite Solar Cells Using Two-Step Sequential Substrate Vibration-Assisted Spray Coating (2S-SVASC)", Nanoscale Research Letters, 2016, 11: 71.

[85] M. I. Asghar, J. Zhang, H. Wang and P. D. Lund, "Devide stability of perovskite solar cells-a review", Renewable and Sustainable Energy Reviews, 2017, 77, 131-146.

[86] L. K. Huang, X. X. Sun, C. Li, R. Xu, J. Xu, Y. Y. Du, Y. X. Wua, J. Ni, H. K. Cai, J. L. Li, Z. Y. Hu and J. J. Zhang, "Electron transport layer-free planar perovskite solar cells: Further performance enhancement perspective from device simulation", Solar Energy Materials and Solar Cells, 2016, Vol. 157, 1038-1047

[87] D. Y. Liu, J. L. Yang, and T. L. Kelly, "Compact Layer Free Perovskite Solar Cells with 13.5% Efficiency" J. Am. Chem. Soc., 2014, 136 (49), 17116–1712

[88] J. Pascual, I. Kosta, T. T. Ngo, A. Chuvilin, G. Cabanero, H. J. Grande, E. M. Barea, I. Mora-, J. L. Delgado and R. Tena-Zaera, "Electron Transport Layer-Free Solar Cells Based on Perovskite–Fullerene Blend Films with Enhanced Performance and Stability" Chemsus Chem. 2016, 9 (18), 2679-2685.

[89] L. L. Zheng, Y. Z. Ma, Y. H. Wang, L. X. Xiao, F. Y. Zhang and H. X. Yang, "Hole Blocking Layer-Free Perovskite Solar Cells with over 15% Efficiency", Energy Procedia 2017(105), 188–193.

[90] W. Q. Wu, Q. Wang, Y. J. Fang, Y. C. Shao, S. Tang, Y. H. Deng, H. D. Lu, Y. Liu, T. Li, Z. B. Yang, A. Gruverman and J. S. Huang, "Molecular doping enabled scalable blading of efficient hole-transport-layer-free perovskite solar cells", Nature Communicationsvolume 2018, (9), Article number: 1625.

[91] T. Liu, L. J. Zuo, T. Ye, J. K. Wu, G. B. Xue, W. F. Fu and H. Z. Chen, "Low temperature processed ITO-free perovskite solar cells without a hole transport layer", RSC Adv., 2015, 5, 94752-94758.

[92] J. L. Duan, Y. Y. Zhao, B. L. He and Q. W. Tang, "Simplified perovskite solar cell with 4.1% efficiency employing inorganic CsPbBr3 as light absorber", Small, 2018, 14, 1704443.

[93] A. Y. Mei, X. Li, L. F. Liu, Z. L. Ku, T. F. Liu, Y. G. Rng, M. Xu, M. hu, J. Z. Chen, Y. Yang, M. Grätzel and H. W. Han, A hole-conductor-free, fully printable mesoscopic perovskite solar cell with high stability, Science, 2014, 345, 295-297.

[94] A. Luque, A. Martí and C. Stanley, "Understanding intermediate-band solar cells", nature photonics, 2012, 6, 146-152. DOI: 10.1038/nphoton.2012.1.

[95] S. Albrecht, M. Saliba, J. P. C Baena, F. Lang, L. Kegelmann, M. Mews, L. Steier, A Abate, J. Rappich, L. Korte, R. Schlatmann, M. K. N azeeruddin, A. Hagfeldt, M. Grätzeld and B. Recha, "Monolithic perovskite/silicon-heterojunction tandem solar cells processed at low temperature", Energy Environ. Sci., 2016, 9, 81-88.

[96] W. M. Wang, J. Yang, X. Zhu and J. Phillips, "Intermediate-band solar cells based on dilute alloys and quantum dots", Front. Optoelectron. 2011, 4 (1): 2–11, DOI 10.1007/s12200-011-0151-z.

[97] D. Shi, Y. Zeng and W. Shen, "Perovskite/c-Si tandem solar cell with inverted nanopyramids: realizing high efficiency by controllable light trapping." Sci. Rep. 2015 (5): 16504. doi: 10.1038/srep16504.

[98] https://www.eurekalert.org/pub_releases/2018-11/hbfm-nri111218.php:"New records in perovskite-silicon tandem solar cells through improved light management"

[99] Y. Okada, N. J. Ekins-Daukes, T. Kita, R. Tamaki, M. Yoshida, A. Pusch, O. Hess, C. C. Phillips, D. J. Farrell, K. Yoshida, N. Ahsan, Y. Shoji, T. Sogabe, and J.-F. Guillemoles, “Intermediate band solar cells: Recent progress and future directions”, Applied Physics Reviews, 2015, 2, 021302-021350.

[100] Y. Zhang, D. L. Geng, X. J. Li, J. Fan, K. Li, H. Z Lian, M. M. Shang and J. Lin, "Wide-Band Excited YTiTaO 6: Eu 3+ /Er 3+ Phosphors: Structure Refinement, Luminescence Properties, and Energy Transfer mechanisms". J. Phys. Chem. C, 2014, 118 (31), pp 17983–17991. DOI: 10.1021/jp504437f.